THE JOURNAL OF BIOLOGICAL CHEMISTRY
Vol. 275, No. 48, Issue of December 1, pp. 37824–37828, 2000

Printed in U.S.A.

Selected Mutations in a Mesophilic Cytochrome *c* Confer the Stability of a Thermophilic Counterpart*

Received for publication, July 5, 2000, and in revised form, July 27, 2000
Published, JBC Papers in Press, July 28, 2000, DOI 10.1074/jbc.M005861200

Jun Hasegawa‡§¶, Susumu Uchiyama¶‖, Yuko Tanimoto‖, Masayuki Mizutani, Yuji Kobayashi‖, Yoshihiro Sambongi‡‡§§, and Yasuo Igarashi****

*From ‡Daiichi Pharmaceutical Co., Ltd., Edogawa-ku, Tokyo 134-8630, Japan, the ‖Faculty of Pharmaceutical Sciences, Osaka University, Suita, Osaka 565-0871, Japan, the **Department of Biotechnology, University of Tokyo, Bunkyo-ku, Tokyo 113-0032, Japan, and the ‡‡Institute of Scientific and Industrial Research, Osaka University, Ibaraki, Osaka 567-0047, Japan*

Mesophilic cytochrome c_{551} of *Pseudomonas aeruginosa* (PA c_{551}) became as stable as its thermophilic counterpart, *Hydrogenobacter thermophilus* cytochrome c_{552} (HT c_{552}), through only five amino acid substitutions. The five residues, distributed in three spatially separated regions, were selected and mutated with reference to the corresponding residues in HT c_{552} through careful structure comparison. Thermodynamic analysis indicated that the stability of the quintuple mutant of PA c_{551} could be partly attained through an enthalpic factor. The solution structure of the mutant showed that, as in HT c_{552}, there were tighter side chain packings in the mutated regions. Furthermore, the mutant had an increased total accessible surface area, resulting in great negative hydration free energy. Our results provide a novel example of protein stabilization in that limited amino acid substitutions can confer the overall stability of a natural highly thermophilic protein upon a mesophilic molecule.

Heat-stable proteins from thermophilic bacteria usually exhibit main chain foldings similar to those of mesophilic counterparts. Mutational studies on mesophilic proteins modeled with respect to thermophilic counterparts have proved that specific side chain interactions in the thermophiles are partially responsible for the higher stability (1–3). Thermodynamic analysis has also indicated that a thermophilic protein can be stabilized through global interaction throughout the molecule (4). It remains enigmatic as to how many amino acid substitutions contribute to the stability of a natural thermophilic protein (5). In some cases, a mesophilic protein only acquires the stability of the thermophilic counterpart after substantial exchanges of a linear sequence; groups of individual mutations are not sufficient (6). Multiple mutations in mesophilic proteins that completely increase the stability to the levels of thermophilic counterparts would provide important information about relationships between local side chain interactions and overall protein stability and demonstrate that the thermophilic character can depend on a limited number of strong noncovalent interactions.

Cytochrome *c* is a powerful tool for characterizing protein stability because structural information on a variety of cytochromes *c* is available, and heterologous expression systems for holopoteins have been established (7). Cytochrome c_{551} (PA c_{551})[1] from a mesophile, *Pseudomonas aeruginosa*, and cytochrome c_{552} (HT c_{552}) from a thermophile, *Hydrogenobacter thermophilus*, are 82- and 80-amino acid proteins, respectively, each with a covalently attached heme. These proteins exhibit 56% sequence identity (8) and almost the same main chain foldings (9), but HT c_{552} exhibits much higher stability compared with PA c_{551} (10). On a structural comparison between HT c_{552} (9) and PA c_{551} (11), we identified three distal regions responsible for the higher stability of the former (9). The single mutation Val-78 to Ile (V78I), and two double mutations Phe-7 to Ala/Val-13 to Met (F7A/V13M) and Phe-34 to Tyr/Glu-43 to Tyr (F34Y/E43Y), chosen with reference to HT c_{552}, in these three regions of PA c_{551} have each been shown to increase protein stability (1).

In the present study, the five mutations were introduced together into PA c_{551}. Thermodynamic analysis showed that the quintuple mutant of PA c_{551} was as stable as HT c_{552}. In order to provide a molecular basis for understanding protein stabilization, we have determined the solution structure of the quintuple mutant. We discuss factors contributing to protein stability in conjunction with structural analyses of HT c_{552}, and the wild-type and quintuple mutant PA c_{551} proteins.

EXPERIMENTAL PROCEDURES

Protein Preparations—Mutations were introduced into the PA c_{551} gene with a polymerase chain reaction-based kit, Mutan-Super Express Km (Takara, Kyoto, Japan), as described previously (1). Transformed *Escherichia coli* JCB7120 cells harboring PA c_{551} genes were harvested from an anaerobic culture, and the proteins used in this study were purified as described previously (1, 8). The concentrations of the purified protein solutions were determined spectrophotometrically using extinction coefficients of ϵ_{551} = 25,200 cm^{-1} M^{-1} and ϵ_{552} = 20,400 cm^{-1} M^{-1} for PA c_{551} and HT c_{552}, respectively. The uniformly ^{15}N- or $^{13}C/^{15}N$-labeled quintuple mutant PA c_{551} protein was obtained from an anaerobic culture with $(^{15}NH_4)_2SO_4$ (99.3%), a ^{15}N-labeled Algal amino

* This work was supported by a grant from the Japanese Ministry of Education, Science and Culture. The costs of publication of this article were defrayed in part by the payment of page charges. This article must therefore be hereby marked "*advertisement*" in accordance with 18 U.S.C. Section 1734 solely to indicate this fact.

The atomic coordinates and structure factors (code 1DVV) have been deposited in the Protein Data Bank, Research Collaboratory for Structural Bioinformatics, Rutgers University, New Brunswick, NJ (http://www.rcsb.org/).

§ To whom correspondence and requests for reprints may be addressed. Tel.: 81-3-3680-0151; Fax: 81-3-5696-8336; E-mail: haseg7li@daiichipharm.co.jp.

¶ These authors contributed equally to this work.

§§ To whom correspondence and reprint requests may be addressed. E-mail: sambongi@sanken.osaka-u.ac.jp.

[1] The abbreviations used are: PA c_{551}, ferrocytochrome c_{551} from *P. aeruginosa*; HT c_{552}, ferrocytochrome c_{552} from *H. thermophilus*; GdnHCl, guanidine hydrochloride; HSQC, heteronuclear single quantum correlation; NOESY, nuclear Overhauser effect spectroscopy; DQF-COSY, double quantum-filtered correlation spectroscopy; DSC, differential scanning calorimetry; ASA, accessible surface area; r.m.s., root mean square.

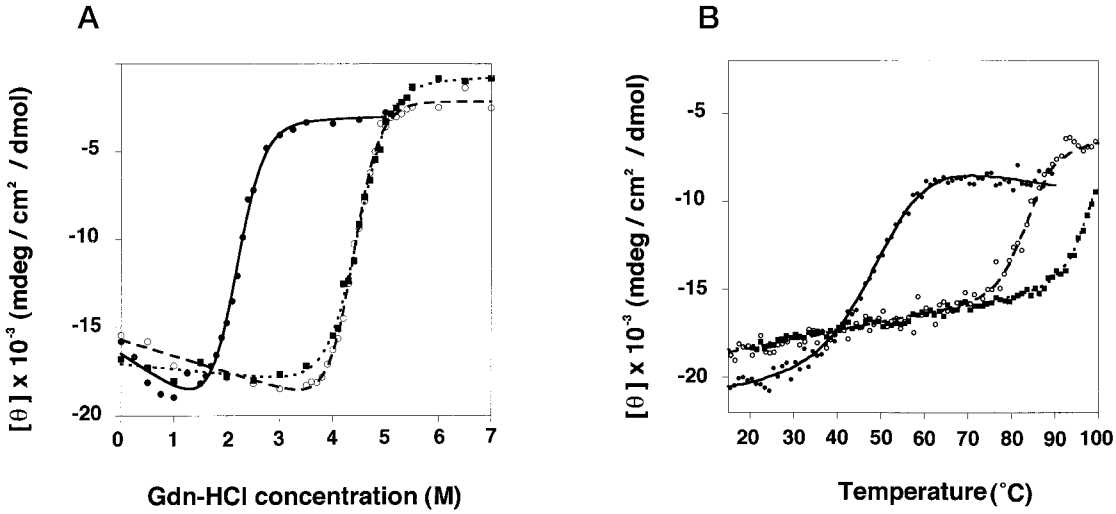

FIG. 1. **Stability of PA c_{551} and HT c_{552} measured by CD.** *A*, chemical denaturation curves induced by GdnHCl measured by CD. The data are plotted as a function of the GdnHCl concentration for the wild-type PA c_{551} (●), the quintuple mutant PA c_{551} (○), and HT c_{552} (■). *B*, thermal denaturation curves observed by CD. The *symbols* are the same as in *A*. The *solid lines* represent the results of nonlinear least-squares best fits based on methods described under "Experimental Procedures."

TABLE I

Thermodynamic parameters characterizing GdnHCl and thermal denaturations

C_m, ΔH_m, and other values were obtained in GdnHCl and thermal denaturation experiments, respectively. ΔH, ΔS, and $\Delta\Delta G$ are the values at T_m of the wild-type PA c_{551} (47.3 °C) estimated from DSC measurements. The hypothetical difference in the free energy change ($\Delta\Delta G_{hyp}$) of the quintuple mutant at the T_m of wild-type PA c_{551} is the sum of the $\Delta\Delta G$ values of the PA c_{551} mutants having the F7A/V13M, F34Y/E43Y, and V78I substitutions. ΔH_m is the calorimetric enthalpy change at T_m of each protein. ΔH_{van} is the van't Hoff enthalpy derived from CD measurements. Errors are estimated from three independent measurements.

Protein	C_m	T_m	ΔH	ΔS	ΔC_P	$\Delta\Delta G$	$\Delta\Delta G_{hyp}$	ΔH_m	ΔH_{van}	ΔT_m
	M	*°C*	*kcal/mol*	*cal/mol/K*	*cal/mol/K*	*kcal/mol*	*kcal/mol*	*kcal/mol*	*kcal/mol*	*°C*
Wild-type PA c-551	2.16 ± 0.03	47.3 ± 0.5	37.7 ± 1.9	118 ± 6	720 ± 40	0		37.7 ± 1.9	35.9 ± 1.8	
Quintuple mutant	4.39 ± 0.02	80.2 ± 0.5	46.0 ± 2.3	125 ± 6	1070 ± 50	5.86 ± 0.29	5.73	80.2 ± 2.4	78.3 ± 3.9	32.9
HT *c*-552	4.47 ± 0.03	87.5 ± 0.5	36.7 ± 1.8	96 ± 5	900 ± 50	6.03 ± 0.30		73.1 ± 3.7	78.3 ± 3.9	40.3

acid mixture (98.2%), and a glycerol-$^{13}C_3$ and $^{13}C/^{15}N$-labeled Algal amino acid mixture (97.5%) as nitrogen and carbon sources. The labeled compounds were obtained from Shoko Co., Ltd. (Tokyo, Japan).

Guanidine Hydrochloride (GdnHCl) Denaturation—Proteins (10 μg/ml) were incubated in diluted HCl water (pH 5.0) with various concentrations of GdnHCl at 25 °C for 2 h before measurements in order to equilibrate the proteins with the denaturant. The CD ellipticity at 222 nm of the protein solutions was measured using a 1-cm path length cuvette at 25 °C with a JASCO J-720 CD spectrophotometer with a PT343 thermoelectric temperature controller. The data were fitted by nonlinear least-squares analysis with KaleidaGraph 3.0 (Synergy Software) employing the Marquart-Levenberg algorithm using a linear extrapolation model as described previously (12). C_m was the concentration of GdnHCl at which the free energy change value, ΔG, became 0.

Thermal Denaturation—The temperature dependence of the CD ellipticity at 222 nm was monitored using a 1-cm path length cuvette with a JASCO J-720 spectrophotometer with a PT343 thermoelectric temperature controller as described previously (1). Protein solutions (~10 μg/ml), pH 5.0, containing 1.5 M GdnHCl were heated from 15 °C to 90 or 100 °C at a heating rate of 1 K/min. Under these conditions, the thermal transition was highly reversible (95%). The van't Hoff enthalpy, ΔH_{van}, was determined from the CD denaturation curve according to a two-state mechanism with a temperature-independent heat capacity change, ΔC_P (13). The ΔC_P values used were obtained by differential scanning calorimetric (DSC) measurements at pH 5.0 in the presence of 1.5 M GdnHCl for each protein. The slope of the CD base line for HT c_{552} in the denatured state was assumed to be the same as that in the native state.

DSC measurements were carried out with the VP-DSC developed by MicroCal Inc. (14). Degassed protein solutions, with a concentration of ~1 mg/ml, were loaded into the calorimeter cell, and each sample was heated from 10 to 125 °C under approximately 3 atmospheres, with a heating rate of 1 K/min. Thermodynamic parameters, *i.e.* T_m, ΔH, ΔS, ΔC_P, and ΔG, were estimated from the heat capacity curve using nonlinear least square fitting based on the previously described method (15, 16). The fitting was performed with MATHEMATICA 3.0 (Wolfram Research Inc.) employing the Marquart-Levenberg algorithm.

NMR Measurement—A protein sample (~1 mM) of the quintuple mutant was dissolved in a 90% H_2O, 10% D_2O or 99.99% D_2O (v/v) solution (pH 5.0 adjusted with HCl), and then reduced with sodium dithionite. All NMR experiments were performed at 25 °C with a Varian UNITYInova 600 spectrometer. Sequential assignments of the backbone resonances of a polypeptide chain were achieved by means of sets of experiments, HNCACB (17), CBCA(CO)NH (18), HNCO (19), (HB)CBCACO(CA)HA (20), and HNHA (21). Protein side chain assignments were made through HCCH-total correlation spectroscopy experiments (22). Stereospecific assignments of the γ-methyl protons of valines and β-methylene protons were made by analyzing HNHB (23), ^{15}N-edited NOESY-HSQC (24), and DQF-COSY (25) spectra. All proton signals from the heme moiety were assigned according to the procedure of Keller and Wüthrich (26). The signals of carbons attached to heme protons were assigned with a constant time ^{13}C-^1H HSQC spectrum (27). All data were processed using the software NMRPipe (28), and the data analysis was assisted by the software PIPP (29). The ^1H, ^{13}C, and ^{15}N resonance assignments of the quintuple mutant have been deposited in the BioMagResBank, under accession number 4578.

Structure Calculation—Approximate interproton distances were obtained from simultaneous $^{13}C/^{15}N$-edited NOESY-HSQC (30), ^{15}N-edited NOESY-HSQC, and NOESY (31) spectra. The mixing time was 60 ms for all NOESY experiments. The distance restraints were grouped into four classes: 1.8–2.7, 1.8–3.3, 1.8–5.0, and 1.8–6.0 Å, corresponding to strong, medium, weak, and very weak NOE cross-peak intensities, respectively. The NOEs including backbone amide protons were grouped into the four classes of 1.8–2.9, 1.8–3.5, 1.8–5.0, and 1.8–6.0 Å. The backbone coupling constants, $^3J_{NH\alpha}$, were measured in a HNHA experiment. The ϕ and ψ-dihedral angle restraints were derived from $^3J_{NH\alpha}$ coupling constants and chemical shift indices. Values of −60 ± 30° and −40 ± 30° were used for the ϕ and ψ-dihedral angles, respectively, for α-helical regions. Hydrogen bond restraints were obtained by analyzing the H/D exchange rates and NOE patterns characteristic of α-helices. Two distance restraints, $r_{NH\text{-}O}$ (0–2.3 Å) and $r_{N\text{-}O}$ (0–3.3 Å),

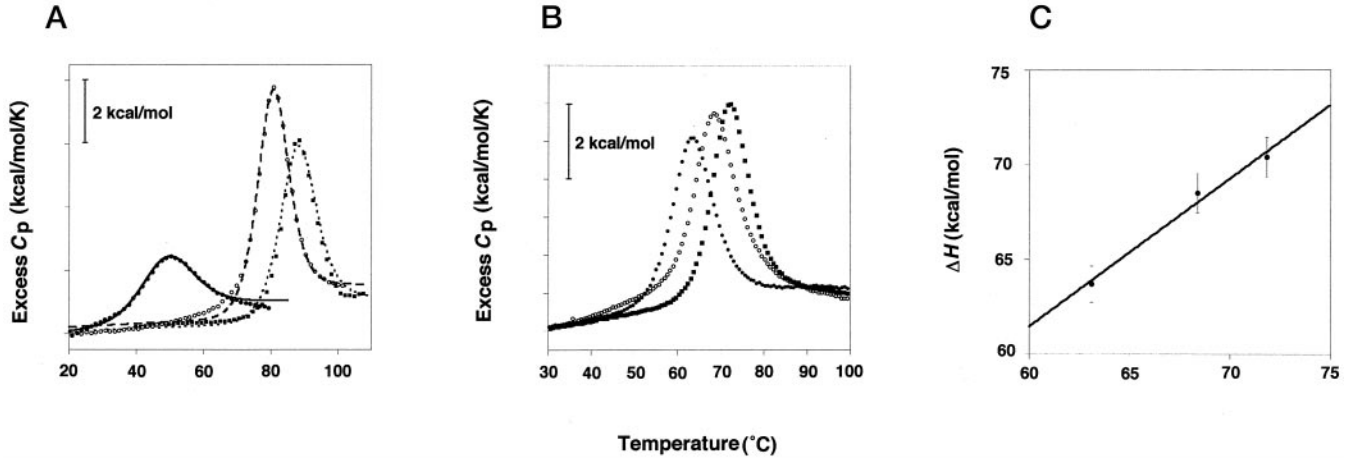

FIG. 2. **DSC analysis of PA c_{551} and HT c_{552}.** *A*, molar heat capacity curves in the presence of 1.5 M GdnHCl observed by DSC for the wild-type PA c_{551} (●), the quintuple mutant PA c_{551} (○), and HT c_{552} (■). The *solid lines* represent the results of nonlinear least-squares best fits based on the two-state model. *B*, heat capacity curves for wild-type PA c_{551} at pH 3.6 (●), 3.8 (○), and 4.0 (■). *C*, enthalpy change of denaturation measured at different pH values *versus* the corresponding denaturation temperature.

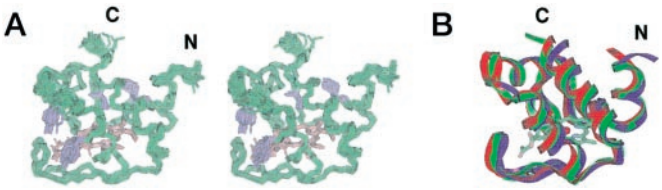

FIG. 3. **Structures of the quintuple mutant and wild-type PA c_{551} proteins and HT c_{552}.** *A*, stereoview of the 20 structures of the quintuple mutant. *B*, schematic representation of main chain folding of the quintuple mutant (*purple*) overlaid with those of the wild-type PA c_{551} (*green*) and HT c_{552} (*red*).

were used for each hydrogen bond. Structures were calculated using the YASAP protocol (32) within X-PLOR 3.1 (33). The coordinates of the quintuple mutant of PA c_{551} have been deposited in the Protein Data Bank, under accession number 1DVV.

Calculation of the Accessible Surface Area (ASA) and Gibbs Free Energy of Hydration for the Native State (G_{hN})—ASA values were calculated using the program MSRoll (34), with a probe radius of 1.4 Å. The Protein Data Bank accession numbers for the three-dimensional structures of the native proteins were 451C and 1AYG for PA c_{551} and HT c_{552}, respectively. Surfaces were classified into polar and nonpolar components by regarding carbon and sulfur atoms as nonpolar and oxygen and nitrogen as polar (35). G_{hN} was calculated according to the method proposed by Oobatake and Ooi (36).

RESULTS AND DISCUSSION

Stability against GdnHCl Denaturation—The far-ultraviolet CD spectrum of the quintuple mutant of PA c_{551} (F7A/V13M/F34Y/E43Y/V78I) was nearly identical to that of the wild type (data not shown). A GdnHCl-induced denaturation curve of the quintuple mutant obtained by CD showed that its C_m value (4.39 M) was highly elevated relative to that of the wild type (Fig. 1*A* and Table I) and essentially the same as that of HT c_{552} (C_m = 4.47 M). Since PA c_{551} and HT c_{552} exhibit a total of 35 amino acid differences, it is noteworthy that only five of these residues are responsible for the enhanced overall stability against chemical denaturation.

Stability against Thermal Denaturation—To address the question of how both the quintuple mutant PA c_{551} and HT c_{552} are thermodynamically stabilized, we performed thermal denaturation experiments using CD and DSC. Fig. 1*B* shows thermal denaturation curves of the quintuple mutant and HT c_{552} together with the wild-type PA c_{551} observed by CD. The ΔH_{van} values estimated from CD measurements for the three proteins were almost identical to the calorimetric enthalpy change at the denaturation temperature (T_m), ΔH_m, obtained from DSC measurements (see below and Table I), indicating that thermal denaturation of these proteins proceeded in a two-state manner.

Fig. 2*A* shows the heat capacity curves of the three proteins measured by DSC. From these curves, thermodynamic parameters were obtained as a function of temperature. We further obtained the ΔC_P value of the wild-type PA c_{551} from T_m-dependent $\Delta H(T_m)$ measurements at pH 3.6, 3.8, and 4.0 in the absence of GdnHCl (Fig. 2, *B* and *C*) (37). The ΔC_P value

TABLE II
Statistics of the 20 structures of the quintuple mutant protein

⟨SA⟩ represents the 20 individual structures calculated with the X-PLOR program. ⟨SA⟩r is the refined structure obtained by energy minimization of the mean structure obtained by simple averaging of the coordinates of the SA structures. F_{NOE} and F_{tor} were calculated using force constants of 50 kcal/mol/Å^2 and 200 kcal/mol/rad^2, respectively. F_{vdw} was calculated using a final value of 4 kcal/mol/Å^2 with the van der Waals hard sphere radii set to 0.75 times those in the parameter set PARALLHSA supplied with the X-PLOR program.

Distance constraints	⟨SA⟩	⟨SA⟩r
Number of violations > 0.3 Å	0	0
r.m.s. deviation from upper bounds (Å)	0.016 ± 0.001	0.015
Angle constraints		
Number of violations > 5 °	0	0
r.m.s. deviation from upper bounds (degrees)	0.102 ± 0.047	0.055
Energy (kcal/mol)		
F_{total}	182.9 ± 1.8	175.31
F_{NOE}	20.02 ± 1.3	17.99
F_{tor}	0.077 ± 0.06	0.018
F_{vdw}	8.71 ± 0.72	9.09
r.m.s. deviation from idealized geometry		
Bonds (Å)	0.003 ± 0.000	0.0026
Angles (degrees)	0.628 ± 0.007	0.63
Impropers (degrees)	0.938 ± 0.096	0.86
Atom r.m.s. deviation (Å)		
⟨SA⟩ *vs.* ⟨SA⟩r		
Residue 3–80 main chain atoms		0.40 ± 0.06
All heavy atoms		0.84 ± 0.05
⟨SA⟩r vs x-ray coordinates of PA c_{551}		
Residue 3–80 main chain atoms		0.84
⟨SA⟩r vs NMR coordinates of HT c_{552}		
Residue 3–78 main chain atoms of HT c_{552}		0.99

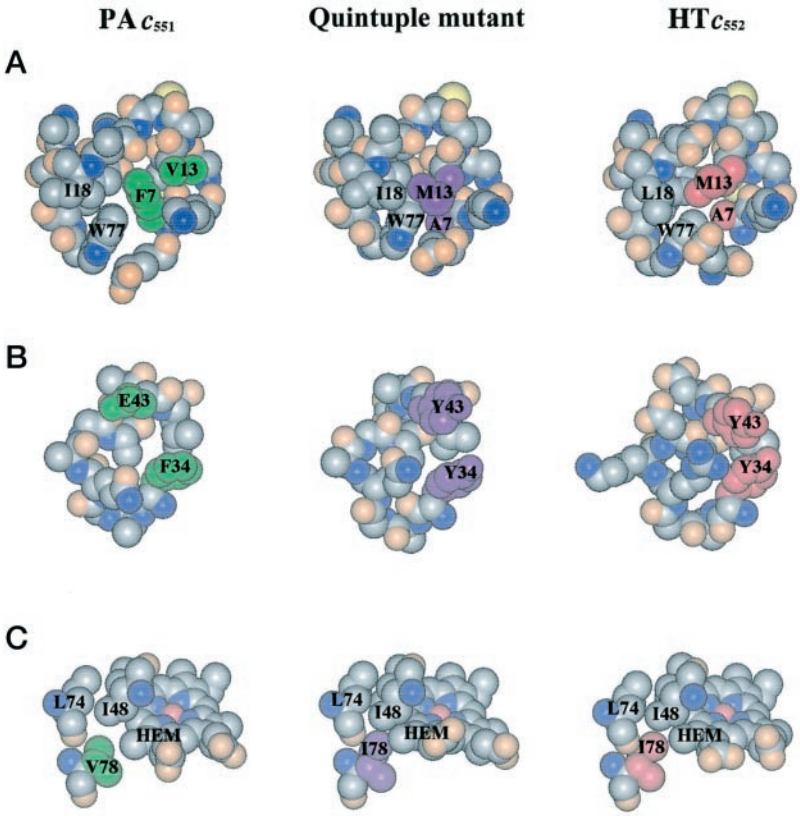

FIG. 4. **Comparison of the side chain packing around the mutation sites in the quintuple mutant and the corresponding regions in the wild-type PA c_{551} and HT c_{552}.** Amino acids mentioned throughout are designated with a one-letter code. Residues in HT c_{552} are shown with the numbering used for those in PA c_{551}. The mutated side chains of the quintuple mutant and the corresponding ones of the wild-type PA c_{551} and HT c_{552} are colored *purple*, *green*, and *red*, respectively. *A*, the hydrophobic region around Phe-7 and Val-13 of the wild-type PA c_{551} and the corresponding regions in the quintuple mutant and HT c_{552}. *B*, the loop and half of the third helix region from Phe-34 to Leu-44 of the wild-type PA c_{551} and the corresponding regions in the quintuple mutant and HT c_{552}. *C*, the internal hydrophobic region around Val-78 and the heme of the wild type and the corresponding regions in the quintuple mutant and HT c_{552}.

TABLE III
Accessible surface area and hydration free energy
ΔG_{hN} was calculated at 298 K.

Protein	ASA	ASA_{pol}	ASA_{np}	ΔG_{hN}
	Å²	*Å²*	*Å²*	*kcal/mol*
Wild-type PA c-551	4434	1906	2528	−82
Quintuple mutant	5013	2653	2460	−167
HT c-552	5377	2663	2714	−180

obtained from the T_m-dependent ΔH value was 781 cal/mol/K, which was close to that obtained on nonlinear fitting of the C_P curve at pH 5.0 in the presence of 1.5 M GdnHCl (720 cal/mol/K; Table I). These results indicate that the ΔC_P values obtained in this study are reliable ones. It has also been reported that the ΔC_P values do not dramatically change in the presence of GdnHCl up to 2.0 M (38).

The DSC measurements (Fig. 2*A*) showed that the quintuple mutant had an increased T_m value of 32.9 °C and enhanced thermodynamic stability ($\Delta\Delta G$) of 5.86 kcal/mol at the T_m value of wild-type PA c_{551} (Table I). These values were nearly the same as those of HT c_{552}. The quintuple mutant exhibited a large increase in ΔH compared with the wild-type PA c_{551} (Table I), suggesting that the mutant was enthalpically stabilized. In contrast, HT c_{552} was stabilized by a small ΔS rather than by an enthalpic factor (Table I). This is obvious from the heat capacity curve (Fig. 2*A*), since the peak height and area (nearly representing ΔH_m) of HT c_{552} were smaller than those of the quintuple mutant although their T_m values were nearly the same. These results suggest that the enhanced T_m values of HT c_{552} and the quintuple mutant are mainly due to the five residues (Ala-7, Met-13, Tyr-34, Tyr-43, and Ile-78, numbered as in the quintuple mutant of PA c_{551}); however, the stabilizing factors differ in the two stable proteins.

Additivity of Thermal Stabilization—We estimated $\Delta\Delta G$ values for the reported PA c_{551} mutants (1) having F7A/V13M, F34Y/E43Y, and V78I substitutions, respectively, by DSC measurements (data not shown). The estimated values were as follows: F7A/V13M, 2.39; F34Y/E43Y, 2.52; and V78I, 0.82 kcal/mol. The $\Delta\Delta G$ value of the quintuple mutant obtained in this study was almost identical to the value for the hypothetical difference in free energy change, $\Delta\Delta G_{hyp}$, *i.e.* the sum of the $\Delta\Delta G$ values for the mutant proteins with the F7A/V13M, F34Y/E43Y, and V78I substitutions, respectively (Table I). This indicates that the mutations in each of the three regions contribute in an additive manner to the enhanced overall stability. The three mutated regions in the quintuple mutant do not interact with each other; thus, they may behave independently without nonlocal structural perturbations.

Structure of the Quintuple Mutant Protein—We next determined the solution structure of the quintuple mutant PA c_{551} protein using 1545 NOE-based distance restraints (comprising 592 intraresidue and intraheme, 300 sequential, 257 medium range, 396 long range including NOEs between the heme and polypeptide chain), supplemented with 102 dihedral and 46 hydrogen bond restraints (Fig. 3*A*). The best 20 structures for the quintuple mutant satisfied the experimental constraints with small deviations from the idealized covalent geometry (Table II). The stereochemical quality of the 20 structures was determined using PROCHECK-NMR (39). Ignoring all glycines and prolines,

98.5% of the remaining residues fell into the most favored and additional allowed regions of ϕ and φ spaces. The average atomic root mean square (r.m.s.) deviations for heavy atoms of residues 3–80 were 0.40 ± 0.06 Å for the main chain atoms and 0.84 ± 0.05 Å for all atoms. These values indicate that the determined structures were well converged and that the restrained energy-minimized structure could be used as a representative for comparison with those of the wild-type PA c_{551} and HT c_{552}. The main chain folding of the quintuple mutant was similar to those of the wild-type PA c_{551} and HT c_{552} (Fig. 3*B*; backbone r.m.s. deviation values were 0.84 Å for residues 3–80 of the wild-type PA c_{551} and 0.99 Å for residues 3–78 of HT c_{552}, respectively). This indicates that the introduction of five mutations into PA c_{551} does not alter the main chain folding.

Structure Comparison between HT c_{552} and the Quintuple Mutant—The structure of the quintuple mutant showed that the side chains of the introduced Ala-7 and Met-13 filled a small cavity found in the wild-type (Fig. 4*A*). The F7A/V13M mutations in this region also changed the Ile-18 side chain conformation to the favorable gauche plus form from the wild-type gauche minus one (Fig. 4*A*). The r.m.s. deviation value for the Ala-7, Met-13, Tyr-27, and Trp-77 heavy chain atoms and the residues 5–20, 25–29, and 75–79 main chain atoms was 1.28 Å when these atoms were superimposed on the corresponding atoms of HT c_{552}.

The two introduced Tyr-34 and Tyr-43 aromatic side chains in the quintuple mutant were adjacent, as found in HT c_{552}, and suggested to undergo a hydrophobic interaction and/or $\pi-\pi$ interaction with one another (Fig. 4*B*). The r.m.s. deviation value for the heavy atoms of the introduced Tyr-34 and Tyr-43 and the main chain atoms of residues 34–44 in the quintuple mutant was 0.91 Å when these atoms were superimposed on the corresponding atoms of HT c_{552}. Molecular modeling of PA c_{551} with the F34Y mutation predicts that the η oxygen atom of the introduced Tyr-34 forms a hydrogen bond with the guanidyl base of Arg-47; this was also indicated by our previous thermodynamic analysis (1). However, it was not clear from the NMR data whether an extra hydrogen bond exists in the quintuple mutant, because the guanidyl base of Arg-47 in the mutant was not well defined in the NMR structure.

The mutant structure also showed that the introduced Ile-78 filled a cavity around the heme, which was found in the wild-type (Fig. 4*C*). The r.m.s. deviation value for the Ile-48, Leu-74, Ile-78, and heme heavy atoms and residues 72–80 main chain atoms in the quintuple mutant was 0.91 Å when these atoms were superimposed on the corresponding atoms of HT c_{552}.

These comparisons of side chain interactions in the three mutated regions of the three proteins clearly showed that the regions in the quintuple mutant became more like those in HT c_{552}.

Difference in Accessible Surface Area—We further evaluated, using the structural data, the effects of the five mutations in the three regions on the total ASA (accessible surface area). The quintuple mutant and HT c_{552} in their native states had larger ASA values compared with that of the wild-type PA c_{551}; this was due to the larger polar ASA (ASA_{pol}) value in both cases (Table III). Thus, undefined hydrophilic and polar groups may be more exposed to the solvent. Consequently, the quintuple mutant and HT c_{552} in the native states exhibited greater negative G_{hN} compared with the wild-type PA c_{551}. The negative G_{hN} values for these two proteins may contribute to the enhanced stability, which is consistent with the results of recent statistical analyses of proteins from thermophiles (40).

Conclusion—Our successful design of a mesophilic protein is, to the best of our knowledge, the first example of protein stabilization to the level of a natural thermophilic counterpart by means of limited amino acid substitutions (2, 41, 42). The formation of extra side chain interactions and exposure of hydrophilic and polar groups of the quintuple PA c_{551} mutant caused the overall elevated stability, which was partly reflected by the increased enthalpy change. The stabilizing strategy for the mutant differed from that in the case of the cold shock protein (43), in which the protein stabilization was mainly achieved through improvement of the electrostatic interaction on the molecular surface.

Our way of carefully comparing the structures of thermophilic and mesophilic homologous proteins and combining selected mutations is valuable for elucidating the relationship between local side chain interactions and overall protein stability. Now that this has been achieved for the first time, it will be worthwhile exploring the possibility of altering other proteins, especially those of industrial and medical interest, in the same manner.

Acknowledgments—We thank R. Muhandirum and L. E. Kay for the pulse sequences and S. J. Ferguson for critical reading of the manuscript.

REFERENCES

1. Hasegawa, J., Shimahara, H., Mizutani, M., Uchiyama, S., Arai, H., Ishii, M., Kobayashi, Y., Ferguson, S. J., Sambongi, Y. & Igarashi, Y. (1999) *J. Biol. Chem.* **274,** 37533–37537
2. Bogin, O., Peretz, M., Hacham, Y., Korkhin, Y., Frolow, F., Kalb (Gilboa), A. J. & Burstein, Y. (1998) *Protein Sci.* **7,** 1156–1163
3. Vetriani, C., Maeder, D. L., Tolliday, N., Yip, K. S., Stillman, T. J., Britton, K. L., Rice, D. W., Klump, H. H. & Robb, F. T. (1998) *Proc. Natl. Acad. Sci. U. S. A.* **95,** 12300–12305
4. Hollien, J. & Marqusee, S. (1999) *Proc. Natl. Acad. Sci. U. S. A.* **96,** 13674–13678
5. Jaenicke, R. & Bohm, G. (1998) *Curr. Opin. Struct. Biol.* **8,** 738–748
6. Eidsness, M. K., Richie, K. A., Burden, A. E., Kurtz, D. M., Jr. & Scott, R. A. (1997) *Biochemistry* **36,** 10406–10413
7. Sambongi, Y., Stoll, R. & Ferguson, S. J. (1996) *Mol. Microbiol.* **19,** 1193–1204
8. Sanbongi, Y., Ishii, M., Igarashi, Y. & Kodama, T. (1989) *J. Bacteriol.* **171,** 65–69
9. Hasegawa J., Yoshida, T., Yamazaki, T., Sambongi, Y., Yu, Y., Igarashi, Y., Kodama, T., Yamazaki, K., Kyogoku, Y. & Kobayashi, Y. (1998) *Biochemistry* **37,** 9641–9649
10. Sanbongi, Y., Igarashi, Y. & Kodama, T. (1989) *Biochemistry* **28,** 9574–9578
11. Matsuura, Y., Takano, T. & Dickerson, R. E. (1982) *J. Mol. Biol.* **156,** 389–409
12. Santoro, M. M. & Bolen, B. W. (1988) *Biochemistry* **27,** 8063–8068
13. Marky, L. & Breslauer, K. (1987) *Biopolymers* **26,** 1601–1620
14. Plotnikov, V. V., Brandts, J. M., Lin, L.-N. & Brandts, J. F. (1997) *Anal. Biochem.* **250,** 237–244
15. Freire, E. (1994) *Methods Enzymol.* **240,** 502–529
16. Sturtevant, J. M. (1987) *Annu. Rev. Phys. Chem.* **38,** 463–488
17. Wittekind, M. & Mueller, L. (1993) *J. Magn. Reson.* **101,** 201–205
18. Grzesiek, A. & Bax, A. (1992) *J. Am. Chem. Soc.* **114,** 6291–6293
19. Kay, L. E., Ikura, M., Tschudin, R. & Bax, A. (1990) *J. Magn. Reson.* **89,** 496–514
20. Kay, L. E. (1993) *J. Am. Chem. Soc.* **115,** 2055–2057
21. Vuister, G. W. & Bax, A. (1993) *J. Am. Chem. Soc.* **115,** 7772–7777
22. Kay, L. E., Xu, G-Y., Singer, A. U., Muhandiram, D. R. & Forman-Kay, J. D. (1993) *J. Magn. Reson. B* **101,** 333–337
23. Archer, S. J., Ikura, M., Torchia, D. A. & Bax, A. (1991) *J. Magn. Reson.* **95,** 636–641
24. Zhang, O., Kay, L. E., Olivier, J. P. & Forman-Kay, J. D. (1994) *J. Biomol. NMR* **4,** 845–858
25. Rance, M., Sørensen, O. W., Bodenhausen, G., Wagner, G., Ernst, R. R. & Wüthrich, K. (1983) *Biochem. Biophys. Res. Commun.* **117,** 479–485
26. Keller, R. M. & Wüthrich, K. (1978) *Biochim. Biophys. Acta* **533,** 195–208
27. Vuister, G. & Bax, A. (1992) *J. Magn. Reson.* **98,** 428–435
28. Delaglio, F., Grzesiek, S., Vuister, G. W., Zhu., G, Pfeifer, J. & Bax, A. (1995) *J. Biomol. NMR* **6,** 277–293
29. Garret, D. S., Powers, R., Gronenborn, A. M. & Clore, G. M. (1991) *J. Magn. Reson.* **95,** 214–220
30. Pascal, S. M., Muhandiran, D. R., Yamazaki, T., Forman-Kay, J. D. & Kay, L. E. (1994) *J. Magn. Reson. B* **103,** 197–201
31. Macura, S. & Ernst, R. R. (1980) *Mol. Phys.* **41,** 95–117
32. Nilges, M., Gronenborn, A. M., Brünger, A. T. & Clore, G. M. (1988) *Protein Eng.* **2,** 27–38
33. Brünger, A. T. (1993) *X-PLOR Version 3.1: A System for X-ray Crystallography and NMR*, Yale University Press, New Haven, CT
34. Connolly, M. L. (1983) *J. Appl. Crystallogr.* **16,** 548–558
35. Richards, F. M. (1977) *Annu. Rev. Biophys. Bioeng.* **6,** 151–176
36. Oobatake, M. & Ooi, T. (1993) *Prog. Biophys. Molec. Biol.* **59,** 237–284
37. Privalov, P. (1979) *Adv. Protein Chem.* **33,** 167–241
38. Makhatadze, G. I. & Privalov, P. L. (1992) *J. Mol. Biol.* **226,** 491–505
39. Laskowski, R. A., Rullmannn, J. A., MacArthur, M. W., Kaptein, R. & Thornton, J. M. (1996) *J. Biomol. NMR* **8,** 477–486
40. Gromiha, M. M., Oobatake, M. & Sarai, A. (1999) *Biophys. Chem.* **82,** 51–67
41. Serrano, L., Day, A. G. & Fersht, A. (1993) *J. Mol. Biol.* **233,** 305–312
42. Malakauskas, S. M. & Mayo, S. L. (1998) *Nat. Struct. Biol.* **5,** 470–475
43. Perl, D., Mueller, U., Heinemann, U. & Schmid, F. X. (2000) *Nat. Struct. Biol.* **7,** 380–383

Selected Mutations in a Mesophilic Cytochrome *c* Confer the Stability of a Thermophilic Counterpart

Jun Hasegawa, Susumu Uchiyama, Yuko Tanimoto, Masayuki Mizutani, Yuji Kobayashi, Yoshihiro Sambongi and Yasuo Igarashi

J. Biol. Chem. 2000, 275:37824-37828.
doi: 10.1074/jbc.M005861200 originally published online July 28, 2000
